ISSN: 3068-7527

Open Access Journal of Medicine and Healthcare

Research Article

OPENPUB GLOBAL PUBLISHERS

Volume 2 | Issue 3

Patient-Level Deep Learning Detection of Invasive Ductal Carcinoma in Breast Histopathology Image Patches Using Explainable Artificial Intelligence

Ahed J Alkhatib*

Department of Legal Medicine, Toxicology and Forensic Medicine, Jordan University of Science & Technology, Jordan.

***Corresponding author:** Ahed J Alkhatib, Department of Legal Medicine, Toxicology and Forensic Medicine, Jordan University of Science & Technology, Jordan.

Citation: Alkhatib, A. J. (2026). Patient-Level Deep Learning Detection of Invasive Ductal Carcinoma in Breast Histopathology Image Patches Using Explainable Artificial Intelligence. Open Access J. Med. Healthc. 2(3). 1-10.

Received: 06-10-2026 **Accepted:** 12-10-2026 **Published:** 20-10-2026

10.5283/OG.OAJMH.17083719

Abstract

Background: Invasive ductal carcinoma (IDC) is the most common type of invasive breast cancer. Diagnosis of IDC is a central task in histopathology. Recent digitization of hematoxylin and eosin stained images has enabled development of deep learning algorithms for detection of cancerous regions. Most studies using image patches as input have a major flaw in that they can have data leakage if patches from the same patient are accidentally present in both training and test set.

Objective: The purpose of this study is to design and assess deep-learning models for classifying breast histopathology image patches as either IDC positive or negative with patient level validation and employing an explainable artificial intelligence approach.

Methods: A secondary analysis of the public Breast Histopathology Images dataset was proposed. The dataset contains 277,524 fifty by fifty pixels RGB image patches of 162 whole-slide breast cancer specimens. The slides were annotated with cancer positive (IDC) and negative. There are 198,738 negative and 78,786 positive patches in the dataset. Patient's ID, coordinates, and class labels were parsed from the file names. The data were split into train, test, and validation sets at the patient level to avoid information leakage. The baseline model was a convolutional neural network. Transfer learning models include VGG16, ResNet50, MobileNetV2, and EfficientNetB0. Accuracy, balanced accuracy, sensitivity, specificity, precision, F1-score, confusion matrix, and ROC-AUC were evaluated. The model's decisions were interpreted using Grad-CAM to visualize the image regions responsible for classification.The expected contribution: The development of a framework for detecting breast cancer from histopathological images at the patch level with patient-level validation and Grad-CAM-based explain ability.

Keywords: Breast Cancer, Invasive Ductal Carcinoma, Histopathology, Deep Learning, Grad Cam, Digital Pathology.

Introduction

Breast cancer stands out as one of the most critical malignancies globally. In 2022, about 2.3 million women were diagnosed with breast cancer, and approximately 670,000 deaths were caused by the disease worldwide [1,2]. Histopathological examination remains fundamental for confirming malignancy, defining tumor type, and supporting treatment planning in breast cancer [3,4]. Invasive breast cancers, particularly invasive ductal carcinomas, constitute a major diagnostic group in which malignant epithelial cells extend beyond the ductal basement membrane into surrounding stromal tissue. Digital pathology has opened new possibilities for computational analysis of breast tissue. Whole-slide imaging allows histological slides to be digitized at high resolution, enabling image-based machine-learning methods to detect morphologic patterns that may assist pathologists [3,5]. Deep learning, particularly convolutional neural networks, has become a central approach in medical image analysis because it can learn spatial and morphological features directly from image pixels [6,7].

Breast histopathology is particularly suitable for artificial-intelligence research because H&E-stained slides contain diagnostically relevant visual information, including nuclear pleomorphism, glandular architecture, stromal invasion, cellular density, and staining patterns [4,8]. Recent reviews show increasing use of deep learning for tumor detection, classification, grading, prediction of molecular biomarkers, prognosis, and treatment-response assessment in breast pathology [4,9-11]. Important challenges remain, including staining variation, limited external validation, class imbalance, interpretability, and the risk of data leakage [5,12-14]. The Breast Histopathology Images dataset is a public database widely used for IDC detection research and was derived from digitized breast-cancer specimens used in earlier IDC-detection work [15]. It consists of 277,524 image patches extracted from 162 whole-slide images, including IDC-negative and IDC-positive patches. File names encode the patient identifier, x-y coordinates, and class label, which permits binary classification, patient-wise splitting, and spatial reconstruction. Patient-wise splitting is critical because random patch-level splitting can place visually related patches from the same patient in both training and test sets, creating information leakage and overoptimistic estimates of generalization [13,14].

The current study, therefore, proposes a patient-level deep-learning framework for IDC detection in breast histopathology patches. Rather than treating the task as a simple patch-classification exercise, the framework emphasizes patient-level separation, standardized model comparison, clinically interpretable performance measures, and explainability through Grad-CAM heatmaps. These elements are consistent with recommendations for transparent and reproducible medical-imaging AI research [13].

Objectives

- To describe distribution of IDC positive and IDC negative histopathology image patches
- To extract patient identifiers, spatial coordinates and class labels from image filename
- To train and compare baseline CNN and transfer-learning based models for binary IDC classification
- To evaluate performance using clinically relevant metrics such as sensitivity, specificity, F1-score and ROC-AUC
- To generate Grad-CAM heatmaps for correct and incorrect classifications in order to improve model interpretability
- To emphasize patient level validation as a safeguard mechanism against data leakage

Methods

Study Design

This study was conceived as a secondary analysis of the public histopathology image set. The approach followed the established methodological guidelines for medical image analysis research, which include transparent reporting of the dataset used, independent validation of findings, use of clinically relevant outcome measures, and emphasis on visual interpretability of results [13].

Dataset

The Breast Histopathology Images dataset contains 277,524 RGB image patches of 50 x 50 pixels derived from 162 whole-slide breast cancer specimens scanned at 40x magnification. Of these, 198,738 patches are IDC-negative and 78,786 are IDC-positive, the class label is encoded in each file name as class0 or class1 [15]. Because multiple patches originate from the same source patient, the effective independent sample size is determined by the number of patients rather than by the raw number of image patches.

Image Labeling and Metadata Extraction

Each image file name comprises a patient ID, x and y coordinates, and class label. The patient ID will be extracted before model development so that no patient can appear in more than one of the training, validation, or test subsets. This grouping is a primary safeguard against data leakage from correlated within-patient image patches [13,14]. The coordinates will be retained for spatial reconstruction of IDC-positive and IDC-negative patch distributions within the source slide. Images will be resized according to the input requirements of each model. The

custom CNN can use the original 50 x 50-pixel patches, whereas transfer-learning models will use dimensions accepted by the selected pretrained architecture, typically 224 x 224 pixels in standard configurations. Resizing changes the numerical input dimensions but does not add histological detail, so the same interpolation procedure should be applied consistently across all subsets. Pixel values will be normalized according to the preprocessing convention of each architecture [16-19]. Training images may undergo histologically plausible data augmentation, including horizontal and vertical flips, limited rotations, and controlled brightness or contrast variation. Augmentation will be applied only to the training subset. H&E color normalization or stain-aware color augmentation may also be considered to reduce technical staining variability, while avoiding excessive normalization that could suppress diagnostically meaningful color differences [12,20].

Data Splitting

A patient-level division will be applied, with patients assigned to training, validation, and test sets. A 70% / 15% / 15% patient allocation is proposed. The exact number of patches in each subset will not necessarily follow the same percentages because patients contribute unequal numbers of patches. The split should be generated before augmentation, and no patch from a given patient may cross subset boundaries. This design reduces leakage and provides a more defensible estimate of performance on unseen patients [13,14].

Model Development

A baseline CNN model will be trained from scratch. Transfer-learning models will include VGG16, ResNet50, MobileNetV2, and EfficientNetB0, representing conventional deep convolution, residual learning, efficiency-oriented inverted residuals, and compound scaling, respectively [16-19]. Pretrained ImageNet weights can be used, followed by fine-tuning of selected upper layers. A sigmoid activation function will be used for binary classification, with binary cross-entropy as the loss function and the Adam optimizer. Early stopping will be based exclusively on validation-set performance.

Model Evaluation

Performance will be evaluated using accuracy, balanced accuracy, sensitivity, specificity, precision, F1-score, and ROC-AUC. Because IDC-positive patches represent the minority class, balanced accuracy, sensitivity, F1-score, and ROC-AUC will be emphasized rather than overall accuracy alone. All final metrics will be calculated on the untouched patient-level test set after model selection has been completed. Where feasible, 95% confidence intervals should be estimated with resampling performed at the patient level rather than by treating correlated patches as fully independent observations [13].

Explainable AI

Grad-CAM will be used to visualize image regions contributing to classification decisions [21]. Heatmaps will be generated for true-positive, true-negative, false-positive, and false-negative examples and overlaid on the corresponding H&E patches. Interpretation will focus on whether highlighted regions overlap with malignant epithelial clusters, stromal interfaces, benign structures, adipose tissue, or technical artifacts. Grad-CAM is a post-hoc attribution method and should not be interpreted as proof that a highlighted region is causally responsible for disease or as a substitute for pathological review [22,23].

Comparative Histological Slides

Figure 1 provides histological orientation for the reader by contrasting representative IDC-negative and IDC-positive H&E-style morphology. In the IDC-negative panels, the expected features include benign ductal or glandular structures, fibrous stroma, and adipose tissue without obvious stromal invasion. In the IDC-positive panels, the intended features include increased epithelial cellularity, nuclear crowding or pleomorphism, irregular malignant nests or clusters, desmoplastic stroma, and disruption of normal architecture. Importantly, the current panel is illustrative rather than an analytic output from the study dataset, it must therefore be replaced by authentic dataset patches before final submission and should not be interpreted as model evidence (Figure 1).

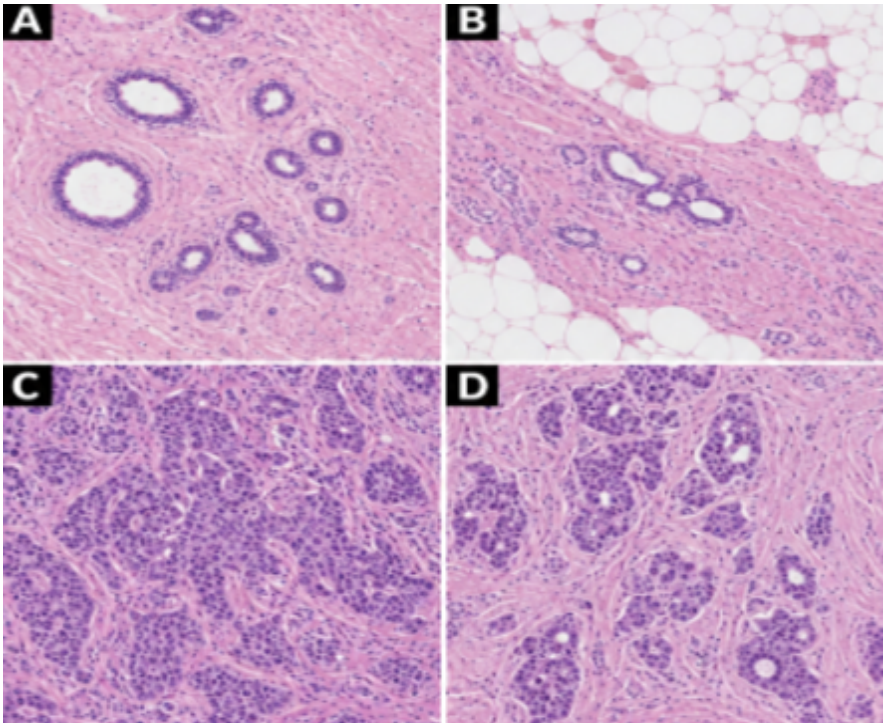


Figure 1: Illustrative Comparative Histological Panel. Panels A and B show IDC-Negative H&E-Style Morphology with Benign Ducts/Glands, Stroma, and Adipose Tissue, Panels C and D show IDC-Positive Invasive Carcinoma-Like Morphology with Increased Cellularity, Irregular Malignant Epithelial Clusters, Stromal Invasion, and Architectural Distortion. This Panel is Provided only for Histological Orientation and Manuscript Layout and Must be Replaced by Authentic Dataset Patches before Final Submission.

Table (1) demonstrates substantial patch-level class imbalance, with IDC-negative patches forming 71.6% of all image patches. This imbalance justifies reporting balanced accuracy, sensitivity, F1-score, and ROC-AUC in addition to raw accuracy. The table should not be interpreted as the prevalence of IDC among patients because the unit shown is the image patch, not the patient.

Table 1: Dataset Distribution by IDC Class

Class	Interpretation	Patches, n	Percentage
Class 0	IDC-negative	198,738	71.6%
Class 1	IDC-positive	78,786	28.4%
Total	All patches	277,524	100.0%

The patient counts in Table (2) are approximate planning values. Because individual patients contribute different numbers of patches, a 70% / 15% / 15% patient split will not necessarily produce the same percentages of patches. The essential rule is that every patch from one patient remains within a single subset, exact patient and patch counts should be reported after grouping by patient ID [13,14].

Table 2: Proposed Patient-Level Data Partition

Subset	Patient allocation	Approximate Patients	Patch allocation	Purpose
Training	70%	113-114	Estimated after patient-level grouping	Model fitting and augmentation.
Validation	15%	24-25	Estimated after patient-level grouping	Hyperparameter tuning and early stopping.
Testing	15%	24-25	Estimated after patient-level grouping	Final unbiased performance estimation.

Table (3) compares architectures with different design goals: VGG16 provides a deep sequential convolutional comparator, ResNet50 introduces residual connections, MobileNetV2 emphasizes computational efficiency through inverted residual blocks, and EfficientNetB0 uses compound scaling [16-19]. Fair comparison requires the same patient split, augmentation policy, evaluation protocol, and model-selection rules across architectures.

Table 3: Candidate Deep-Learning Architectures

Model	Input strategy	Main role	Comment
Baseline CNN	50 x 50 or resized patches	Reference model	Trained from scratch to provide a simple benchmark.
VGG16	Resized patches	Transfer learning	Deep sequential convolutional architecture, useful comparator.
ResNet50	Resized patches	Transfer learning	Residual architecture, often strong in image classification.
MobileNetV2	Resized patches	Efficient transfer learning	Lower computational burden, useful for deployment-oriented analysis.
EfficientNetB0	Resized patches	Efficient transfer learning	Compound scaling, strong accuracy-efficiency balance.

Table (4) is a results template and does not yet contain empirical model performance. The completed table should report only metrics obtained from the untouched patient-level test set. Sensitivity equals TP/(TP+FN), specificity equals TN/(TN+FP), precision equals TP/(TP+FP), and F1-score is the harmonic mean of precision and sensitivity. Classification thresholds should be selected using training/validation data rather than optimized on the final test set, 95% confidence intervals are recommended where feasible [13].

Table 4: Comparative Model Performance Template

Model	Accuracy	Balanced accuracy	Sensitivity	Specificity	Precision	F1-score	ROC-AUC
Baseline CNN	Pending	Pending	Pending	Pending	Pending	Pending	Pending
VGG16	Pending	Pending	Pending	Pending	Pending	Pending	Pending
ResNet50	Pending	Pending	Pending	Pending	Pending	Pending	Pending
MobileNetV2	Pending	Pending	Pending	Pending	Pending	Pending	Pending
EfficientNetB0	Pending	Pending	Pending	Pending	Pending	Pending	Pending

Note: This table should be completed after model training using the independent patient-level test set.

Figure 2. Class Distribution

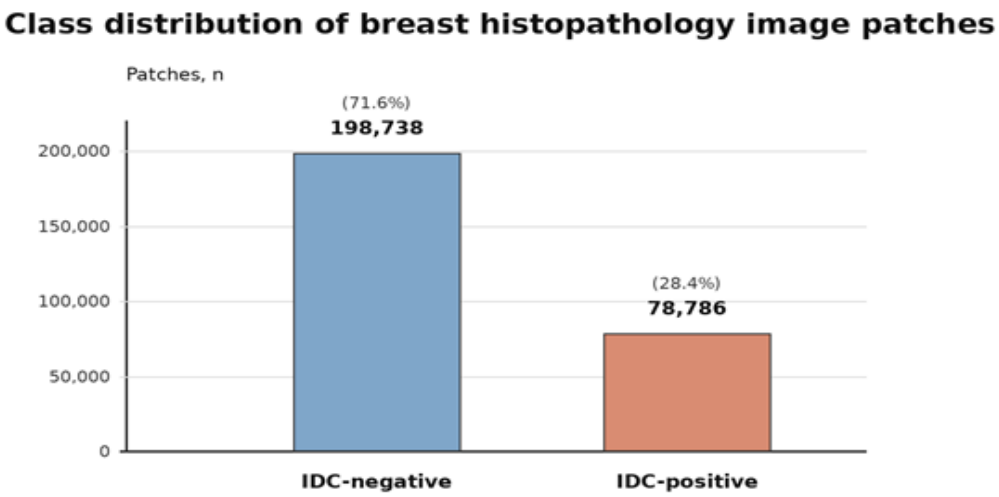


Figure 2. Class distribution of IDC-negative and IDC-positive image patches in the public breast histopathology dataset. The chart shows patch-level counts (198,738 negative and 78,786 positive) and demonstrates the approximately 72:28 class imbalance. These percentages describe image patches, not patient-level prevalence, because each patient contributes multiple patches. Figures (3-6). Figures 3-6 are intentionally presented as templates because model training and independent testing have not yet been completed. They should be replaced with empirical outputs before the manuscript is presented as a completed original research article. Until then, these elements describe the planned reporting structure rather than observed results.

Expected Results

The data set is likely to exhibit class imbalance. For instance, IDC-negative patches are expected to account for roughly 72% of the data set, while positive patches would account for the remaining 28%. The use of transfer-learning models is likely to be preferable to a naïve CNN since pretrained networks have been demonstrated to offer relevant hierarchical image features, which can serve as building blocks for the solution, however, this is an empirical claim, which must be supported by evidence. Performance on patient-

level splits is expected to be lower compared to estimates that used random patch-level splits because patient-level separation will reduce the risk that patches belonging to the same patient will appear in both development and validation sets [14]. Such an outcome would be a more realistic generalization error than the one implied by the random splits. Model outputs should be presented using complementary numerical tables and visual figures. Table (4) should be reserved for summarizing test-set performance only after all models have been finalized. Confusion matrices will make the pattern of false-positive and false-negative errors explicit, and ROC curves will compare discrimination across thresholds, but the training/validation curves will document optimization behavior. Grad-CAM panels will provide a qualitative check of whether the model has attention overlapping with histologically meaningful regions, but with the caveat that attribution maps should be cautiously interpreted with pathological insight [13,21].

Discussion

This study tackles a challenging task of classification of IDC-positive and IDC-negative breast histology patches with reduced methodological bias. Notably, while the data set is large at the patch level, it is relatively small at the patient level. This is why patient-level validation is critical, since patches from the same patient are likely to be confounded by staining, scanning, preparation, or other factors specific to the case. In other words, if two patches originate from the same patient, their association with positive or negative outcome may stem not from general applicability but from specific circumstances of that particular case [13,14].

The proposed analysis has several strengths that include the following:

First, the analysis utilizes a large publicly available dataset whose labels are well-encoded. Second, the study benchmarks a baselines CNN architecture against several well-established transfer-learning-based approaches and not just one model [16-19]. Third, it reports performance using clinically relevant metrics beyond accuracy. Fourth, it leverages Grad CAM visualization to probe whether the model attends to the expected histopathological regions as a step toward enhancing model interpretations, a crucial factor for the success of deep learning [21,23-25]. The histological comparison between IDC-negative and IDC-positive patches is also important, since IDC-negative patches may contain benign ducts, stromal tissue, fat, or regions of non-invasive tissue, while IDC-positive patches should contain invasive malignant epithelial clusters, nuclear atypia, increased cellularity, and disruption of normal tissue architecture [4,8]. The model should therefore be evaluated not only in terms of numerical accuracy, but also in terms of whether its spatial attention is compatible with these features. False classifications are especially insightful, since they may indicate overlapping of morphologic categories, small foci of tumor, a lack of contextual information, or attention to non-biological artifacts in the images.

Interpretive Caution for Explain Ability

The Grad-CAM algorithm allows the visualizing of the regions in an image where a convolutional network concentrated class-related activation, however, the spatial map appears to be relatively coarse and could change depending on the model architecture/layers chosen. Thus, a visually plausible heatmap should be seen as supportive evidence of model behavior rather than proof of pathological reasoning. Review of both correct and incorrect classifications is important for finding possible shortcut features and determining if explanations are consistent with recognizable breast histology [21,22]. The study also had a number of limitations. The data used was patch-based, which does not include clinical metadata, tumor grade, receptor status, molecular subtype, treatment, and survival information, and therefore the model is not a complete diagnostic system. The 50×50 pixel patch size may also be too small to capture context for cases, where stromal invasion or tumor margins need to be considered at a larger scale. Furthermore, the staining or scanners from the original dataset may impact the ability of the model to generalize to other laboratories, despite augmentation and normalization. To further evaluate the claim, the analysis could have integrated an external validation set on a different breast histopathology image dataset, such as BACH or Break His [26,27].

Conclusion

This manuscript describes a novel patient-level deep-learning methodology for the detection of invasive ductal carcinoma in breast histopathology image patches that employs comparative histological visualization, transfer-learning model validation, rigorous

patient-level assessment, and grad-cam-based model explanation. The study, if executed properly and reported with methodological rigor, represents a highly valuable contribution to the literature in digital breast pathology and computer-aided cancer diagnosis.

Ethical Considerations

This study utilizes a publicly available and de-identified image set, and involves no direct interaction with human participants. Institutional review board exemption may be appropriate for this study, depending on the policies of the participating institutions. The manuscript should note that all analyses were conducted on anonymized public data, and that no private patient information was accessed.

Conflict of Interest

The author declares no conflict of interest.

References

1. World Health Organization. (2026). Breast cancer fact sheet. World Health Organization.
2. Bray, F., Laversanne, M., Sung, H., Ferlay, J., Siegel, R. L., Soerjomataram, I., & Jemal, A. (2024). Global cancer statistics 2022: GLOBOCAN estimates of incidence and mortality worldwide for 36 cancers in 185 countries. CA: a cancer journal for clinicians, 74(3), 229-263.
3. Pantanowitz, L., Sharma, A., Carter, A. B., Kurc, T., Sussman, A., & Saltz, J. (2018). Twenty years of digital pathology: an overview of the road travelled, what is on the horizon, and the emergence of vendor-neutral archives. Journal of pathology informatics, 9(1), 40.
4. Soliman, A., Li, Z., & Parwani, A. V. (2024). Artificial intelligence's impact on breast cancer pathology: a literature review. Diagnostic pathology, 19(1), 38.
5. Tizhoosh, H. R., & Pantanowitz, L. (2018). Artificial intelligence and digital pathology: challenges and opportunities. Journal of pathology informatics, 9(1), 38.
6. Janowczyk, A., & Madabhushi, A. (2016). Deep learning for digital pathology image analysis: A comprehensive tutorial with selected use cases. Journal of pathology informatics, 7(1), 29.
7. Litjens, G., Kooi, T., Bejnordi, B. E., Setio, A. A. A., Ciompi, F., Ghafoorian, M., ... & Sánchez, C. I. (2017). A survey on deep learning in medical image analysis. Medical image analysis, 42, 60-88.
8. Khan, A. M., Sirinukunwattana, K., & Rajpoot, N. (2015). A global covariance descriptor for nuclear atypia scoring in breast histopathology images. IEEE journal of biomedical and health informatics, 19(5), 1637-1647.
9. Jiang, B., Bao, L., He, S., Chen, X., Jin, Z., & Ye, Y. (2024). Deep learning applications in breast cancer histopathological imaging: diagnosis, treatment, and prognosis. Breast Cancer Research, 26(1), 137.
10. McCaffrey, C., Jahangir, C., Murphy, C., Burke, C., Gallagher, W. M., & Rahman, A. (2024). Artificial intelligence in digital histopathology for predicting patient prognosis and treatment efficacy in breast cancer. Expert review of molecular diagnostics, 24(5), 363-377.
11. Priya CV, L., VG, B., BR, V., & Ramachandran, S. (2024). Deep learning approaches for breast cancer detection in histopathology images: A review. Cancer Biomarkers, 40(1), 1-25.

12. Tellez, D., Litjens, G., Bándi, P., Bulten, W., Bokhorst, J. M., Ciompi, F., & Van Der Laak, J. (2019). Quantifying the effects of data augmentation and stain color normalization in convolutional neural networks for computational pathology. Medical image analysis, 58, 101544.

13. Mongan, J., Moy, L., & Kahn Jr, C. E. (2020). Checklist for artificial intelligence in medical imaging (CLAIM): a guide for authors and reviewers. Radiology: Artificial Intelligence, 2(2), e200029.

14. Kapoor, S., & Narayanan, A. (2023). Leakage and the reproducibility crisis in machine-learning-based science. Patterns, 4(9).

15. Cruz-Roa, A., Basavanhally, A., González, F., Gilmore, H., Feldman, M., Ganesan, S., ... & Madabhushi, A. (2014, March). Automatic detection of invasive ductal carcinoma in whole slide images with convolutional neural networks. In Medical imaging 2014: Digital pathology (Vol. 9041, p. 904103). SPIE.

16. Simonyan, K., & Zisserman, A. (2014). Very deep convolutional networks for large-scale image recognition. arXiv preprint arXiv:1409.1556.

17. He, K., Zhang, X., Ren, S., & Sun, J. (2016). Deep residual learning for image recognition. In Proceedings of the IEEE conference on computer vision and pattern recognition (pp. 770-778).

18. 18. Sandler, M., Howard, A., Zhu, M., Zhmoginov, A., & Chen, L. C. (2018, June). Mobilenetv2: Inverted residuals and linear bottlenecks. In 2018 IEEE/CVF conference on computer vision and pattern recognition (pp. 4510-4520). Ieee.

19. Tan, M., & Le, Q. (2019, May). Efficientnet: Rethinking model scaling for convolutional neural networks. In International conference on machine learning (pp. 6105-6114). PmLR.

20. Macenko, M., Niethammer, M., Marron, J. S., Borland, D., Woosley, J. T., Guan, X., ... & Thomas, N. E. (2009, June). A method for normalizing histology slides for quantitative analysis. In 2009 IEEE international symposium on biomedical imaging: from nano to macro (pp. 1107-1110). IEEE.

21. Selvaraju, R. R., Cogswell, M., Das, A., Vedantam, R., Parikh, D., & Batra, D. (2017). Grad-cam: Visual explanations from deep networks via gradient-based localization. In Proceedings of the IEEE international conference on computer vision (pp. 618-626).

22. Chattopadhay, A., Sarkar, A., Howlader, P., & Balasubramanian, V. N. (2018, March). Grad-cam++: Generalized gradient-based visual explanations for deep convolutional networks. In 2018 IEEE winter conference on applications of computer vision (WACV) (pp. 839-847). IEEE.

23. Abdullakutty, F., Akbari, Y., Al-Maadeed, S., Bouridane, A., Talaat, I. M., & Hamoudi, R. (2024). Histopathology in focus: a review on explainable multi-modal approaches for breast cancer diagnosis. Frontiers in Medicine, 11, 1450103.

24. Ragab, D. A., Sharkas, M., Marshall, S., & Ren, J. (2019). Breast cancer detection using deep convolutional neural networks and support vector machines. PeerJ, 7, e6201.

25. Chaudhury, S., Sau, K., Khan, M. A., & Shabaz, M. (2023). Deep transfer learning for IDC breast cancer detection using fast AI technique and Sqeezenet architecture. Math Biosci Eng, 20(6), 10404-10427.

26. Aresta, G., Araújo, T., Kwok, S., Chennamsetty, S. S., Safwan, M., Alex, V., ... & Aguiar, P. (2019). Bach: Grand challenge on breast cancer histology images. Medical image analysis, 56, 122-139.

27. Spanhol, F. A., Oliveira, L. S., Petitjean, C., & Heutte, L. (2015). A dataset for breast cancer histopathological image classification. Ieee transactions on biomedical engineering, 63(7), 1455-1462.

28. Eskandari, S., Eslamian, A., & Cheng, Q. (2024). Comparative analysis of transfer learning models for breast cancer classification. arXiv preprint arXiv:2408.16859.

29. Howard, A. G., Zhu, M., Chen, B., Kalenichenko, D., Wang, W., Weyand, T., ... & Adam, H. (2017). Mobilenets: Efficient convolutional neural networks for mobile vision applications. arXiv preprint arXiv:1704.04861.

30. Kohl, M., Walz, C., Ludwig, F., Braunewell, S., & Baust, M. (2018, June). Assessment of breast cancer histology using densely connected convolutional networks. In International conference image analysis and recognition (pp. 903-913). Cham: Springer International Publishing.

31. 31. Mahmud, M. I., Mamun, M., & Abdelgawad, A. (2023, March). A deep analysis of transfer learning based breast cancer detection using histopathology images. In 2023 10th International Conference on Signal Processing and Integrated Networks (SPIN) (pp. 198-204). IEEE.

32. Nakach, F. Z., Idri, A., & Goceri, E. (2024). A comprehensive investigation of multimodal deep learning fusion strategies for breast cancer classification. Artificial Intelligence Review, 57(12), 327.

33. Perez-Nunez, J. R., Rodriguez, C., Vasquez-Serpa, L. J., & Navarro, C. (2024). The challenge of deep learning for the prevention and automatic diagnosis of breast cancer: a systematic review. Diagnostics, 14(24), 2896.

34. Ronneberger, O., Fischer, P., & Brox, T. (2015, October). U-net: Convolutional networks for biomedical image segmentation. In International Conference on Medical image computing and computer-assisted intervention (pp. 234-241). Cham: Springer international publishing.

35. Shiri, M., Reddy, M. P., & Sun, J. (2024, August). Supervised contrastive vision transformer for breast histopathological image classification. In 2024 IEEE international conference on information reuse and integration for data science (IRI) (pp. 296-301). IEEE.

36. Tafavvoghi, M., Bongo, L. A., Shvetsov, N., Busund, L. T. R., & Møllersen, K. (2024). Publicly available datasets of breast histopathology H&E whole-slide images: A scoping review. Journal of Pathology Informatics, 15, 100363.

37. Valencia-Duque, A. F., Cardenas-Peña, D. A., Gil-González, J., Orozco-Gutiérrez, Á., & Daza-Santacoloma, G. (2024, July). Breast Cancer Tissue Classification from Multiple Annotators using Chained Deep Learning Approaches. In 2024 46th Annual International Conference of the IEEE Engineering in Medicine and Biology Society (EMBC) (pp. 1-4). IEEE.

38. Vang, Y. S., Chen, Z., & Xie, X. (2018, June). Deep learning framework for multi-class breast cancer histology image classification. In International conference image analysis and recognition (pp. 914-922). Cham: Springer International Publishing.

39. Wang, W., Li, Y., Yan, X., Xiao, M., & Gao, M. (2024, September). Breast cancer image classification method based on deep transfer learning. In Proceedings of the International Conference on Image Processing, Machine Learning and Pattern Recognition (pp. 190-197).

40. Wang, X., & Yuan, W. (2024). Nuclei-level prior knowledge constrained multiple instance learning for breast histopathology whole slide image classification. Iscience, 27(6).

Copyright:©2026 Ahed J Alkhatib. an open-access article distributed under the terms of the Creative Commons Attribution License, which permits unrestricted use, distribution, and reproduction in any medium, provided the original author and source are credited.